Journal of Nuclear Materials 471 (2016) 154–164

Contents lists available at ScienceDirect

Journal of Nuclear Materials

journal homepage: www.elsevier.com/locate/jnucmat

Modeling the homogenization kinetics of as-cast U-10wt% Mo alloys

Zhijie Xu [a, *], Vineet Joshi [c], Shenyang Hu [b], Dean Paxton [d], Curt Lavender [c], Douglas Burkes [d]

[a] Computational Mathematics Group, Pacific Northwest National Laboratory, Richland, WA 99352, USA
[b] Reactor Materials & Mechanical Design, Pacific Northwest National Laboratory, Richland, WA 99352, USA
[c] Energy Processes & Materials Division, Pacific Northwest National Laboratory, Richland, WA 99352, USA
[d] Nuclear Engineering and Analysis Group, Pacific Northwest National Laboratory, Richland, WA 99352, USA

ARTICLE INFO

Article history:
Received 3 April 2015
Received in revised form
5 September 2015
Accepted 16 November 2015
Available online 15 January 2016

Keywords:
Uranium
Molybdenum
Homogenization modeling
Diffusion
Microstructure characterization
BSE-SEM

ABSTRACT

Low-enriched U-22at% Mo (U–10Mo) alloy has been considered as an alternative material to replace the highly enriched fuels in research reactors. For the U–10Mo to work effectively and replace the existing fuel material, a thorough understanding of the microstructure development from as-cast to the final formed structure is required. The as-cast microstructure typically resembles an inhomogeneous microstructure with regions containing molybdenum-rich and -lean regions, which may affect the processing and possibly the in-reactor performance. This as-cast structure must be homogenized by thermal treatment to produce a uniform Mo distribution. The development of a modeling capability will improve the understanding of the effect of initial microstructures on the Mo homogenization kinetics. In the current work, we investigated the effect of as-cast microstructure on the homogenization kinetics. The kinetics of the homogenization was modeled based on a rigorous algorithm that relates the line scan data of Mo concentration to the gray scale in energy dispersive spectroscopy images, which was used to generate a reconstructed Mo concentration map. The map was then used as realistic microstructure input for physics-based homogenization models, where the entire homogenization kinetics can be simulated and validated against the available experiment data at different homogenization times and temperatures.

1. Introduction

Enriched uranium (>90% ^{235}U) has been widely used in many nuclear applications where high fissile material density is needed. The proliferation concern associated with the use of highly enriched uranium (HEU: enrichment >20% ^{235}U) motivates the U.S. Department of Energy's (DOE's) United States High Performance Research Reactor (USHPRR) Conversion Program to seek low-enriched uranium (LEU) alternatives. The conversion of HEU research reactors to the use of LEU requires an increase in the total density of uranium atoms in the fuel. The previous scoping studies identified uranium–molybdenum (U–Mo) alloys with Mo concentration 7–10 wt% as promising candidate materials for LEU fuel because of their favorable attributes under irradiation and high intrinsic uranium density [1,2]. Gamma-phase U with Mo in solid solution possesses acceptable irradiation stability, good mechanical properties and corrosion resistance, and can be formed over a wide range of Mo concentration.

Two forms of U–Mo alloy fuel plates have been investigated and tested under the USHPRR Conversion Program: a dispersion fuel with fuel particles dispersed in an aluminum matrix, and a monolithic fuel in aluminum alloy cladding [2,3]. The fuel plate assembly consists of a central layer (fuel meat with U–Mo alloy) sandwiched between cladding sheets, and is manufactured by various hot and cold rolling processes.

Complex materials processing techniques including casting, thermal annealing, hot and cold rolling, coating, and hot isostatic pressing (HIP) are used to fabricate U–Mo metallic fuel plates. Based on the earlier work [1–7] on the thermomechanical processing of U–10Mo it was determined that different combinations and sequences of material processes may result in a variety of microstructures with different Mo segregation, grain morphology, phase volume fractions, carbide inclusions, and so on. In order to fabricate U–10Mo monolithic plates consistently, at a lower cost and with high yield, a thorough understanding of the microstructure evolution kinetics from as-cast to the final formed

* Corresponding author.
E-mail address: zhijie.xu@pnnl.gov (Z. Xu).

http://dx.doi.org/10.1016/j.jnucmat.2015.11.026
0022-3115/

structure after various material processes is required. The U–10Mo as-cast microstructure is an inhomogeneous dendritic structure with molybdenum-rich and -lean regions [4–7]. It has been observed in U–10Mo that, depending on the casting process adopted [5], microstructures with different grain size, molybdenum inhomogeneity, secondary dendrite arm spacing and carbide distribution were observed. Mo segregation during casting may affect γ phase stability and the formation of α phase as well as the phase transition from γ to α and γ' during thermal annealing. A homogenization process is needed to alleviate Mo segregation and produce desired microstructures with uniformly distributed Mo. Homogenization of U–10Mo is performed in the γ-phase field (above 560 °C) for several hours [7–9]. The kinetics of the homogenization is dependent on the grain size and the other aforementioned parameters, and experimentally determining the time and temperature to homogenize is time-consuming and labor-intensive. Recent work on homogenization of U–10Mo was performed by Leenaers [7] and Joshi et al. [4–6]. The homogeneity or inhomogeneity was observed using the x-ray techniques in scanning electron microscope (SEM). The as-cast samples in these cases were annealed for several hours and the microstructure was observed for inhomogeneity. In order to overcome this heuristic approach, a homogenization model is necessary to predict the kinetics for varied grain sizes. Computational modeling combined with experimental validation will improve understanding of microstructural evolution kinetics and make it possible to improve the alloy design with optimized process parameters to achieve desired microstructures and material properties.

Prior work involving the modeling of the homogenization kinetics in the as-cast U–10Mo does not exist; however preliminary work involving U–Nb alloy work was performed by Snyder in 1978 [10,11] and more recently by Lopez et al. on U-7.5Nb-2.5Zr [12] alloys. These models used scanning electron microscope (SEM) energy dispersive spectroscopy (EDS) line scans and microhardness measurements to determine the degree of inhomogeneity. A simple analytical model [13] was used by Snyder [6] to determine the time required to homogenize the entire casting. Despite the ease of using this model, that work does not take into account the variability associated with the entire microstructure or is localized to the regions where the line scans are taken and the step size of the scans. A better way to include the entire microstructure is to perform microprobe analysis on the entire image (wavelength dispersive spectroscopy [WDS] maps). This technique, though reliable, is tedious and time-consuming, and techniques that better correlate the microstructure with chemistry are required. Other techniques based on phase field, calculation of phase diagrams, etc. [14–18], to simulate the homogenization kinetics for different alloys are present in the literature [19–21]. These techniques use special tools or software that usually require a specialist and resources that are uncommon in the production environment.

The objective of this paper is to present a homogenization model of the U–10Mo alloy. To model the homogenization of U–10Mo, transport processes taking place in the metal, along the grain boundary, and from bulk alloy to grain boundary must be considered in detail. Such transport processes should have important roles in defining the overall kinetic rate of homogenization. The paper is organized as follows: an experimental study of homogenization in U–10Mo is presented first in Section II, followed by description of a modeling study of homogenization kinetics in Section III. Section IV applies the proposed model to homogenization of U–10Mo with results and discussion. Connections to experiments are presented where possible, and conclusions are drawn in Section V.

2. Homogenization studies for Idaho National Laboratory (INL) pin casting samples

2.1. Experimental procedure

For the current work, U–10Mo samples were machined from 38.1 mm-long by 6.35 mm-diameter pins that had been arc melted and cast into copper molds at INL, Idaho Falls, USA. The feedstock used in the arc melting was in the form of pieces sectioned from a coupon that had been machined from a vacuum-induction-melted and cast plate of U–10Mo. The plate was melted at 1330 °C, cast into a graphite mold and homogenized in-mold at 1100 °C for 4 h. All materials processing, other than that performed at INL, was conducted at the Y-12 National Security Complex, Oak Ridge, USA. The bulk chemical composition of the arc-cast samples was not measured; however, the composition of the coupon was determined to be U 88.7 wt% (99.8 wt% ^{238}U), Mo 10.1 wt%, C 0.08 wt%, and Si 0.04 wt%, with Al, Co, W and Cu accounting for less than 1.5 wt%. The homogenization heat treatments were conducted in a high-temperature vacuum furnace (MTI Model VBF-1200X) operated under inert atmosphere using high-purity bottled argon. The atmospheric flow rate was maintained at approximately 11.7×10^{-6} m^3/s. The samples were wrapped in Zr foil and placed in an alumina crucible (with lid). The furnace was evacuated and backfilled with argon three times; then continuous argon flow was used to establish a slight positive pressure. The heating cycle used a 10 °C/min ramp rate to 350 °C, a 15 min hold, and another ramp at the same rate to the homogenization temperature for the required amount of time, i.e., 4–48 h. This was followed by furnace cooling under flowing argon back to room temperature. The cooling rate was approximately 25 °C/min.

For the microstructural characterization, samples were cold-mounted in an epoxy resin and then sectioned at approximately half the length. The mounted samples were successively polished down to 600 grit with SiC polishing papers and were further polished using 6 μm and 1 μm diamond slurries, followed by a final colloidal silica polish. Upon polishing, the samples were gold coated for SEM analysis. The detailed technique used to prepare the samples for characterization can be found elsewhere [22]. Microstructural characterization was performed using an optical microscope as well as using a JEOL JSM-7600F SEM equipped with an Oxford Instruments X-Max 80 EDS detector. The EDS analysis was performed using the INCA Microanalysis Suite software, version 4.15. For the line scan analysis, the heat-treated samples were imaged at 500 × in backscattered electron (BSE-SEM) mode to highlight the atomic number contrast (Z contrast). Three EDS line scans of 225 μm length were performed at random regions. The line scans were used to count the molybdenum content for 30 s at an interval of 0.9 μm. Due to the presence of carbides and oxygen in the system, the EDS line scans also involved detecting these elements. Due to rapid oxidation of the surface of the U–10Mo sample upon polishing and the presence of adventitious carbon and the small interaction volume of the electron beam; the composition of the molybdenum is skewed. However this being a systematic error will not affect the eventual data.

2.2. Results (800 °C and 1000 °C): BSE-SEM images and line scan data

In order to determine the time and temperature required to transform the cast structure to the homogenized structure, a series of heat treatments were conducted. The samples were homogenized at 800 °C for 4, 8, 16, 24 and 48 h [23]. Fig. 1a, b, c are the typical as-cast, 800 °C for 4 h, and 800 °C for 24 h, respectively, of U–10Mo alloy in the BSE-SEM mode. The chemical homogeneity

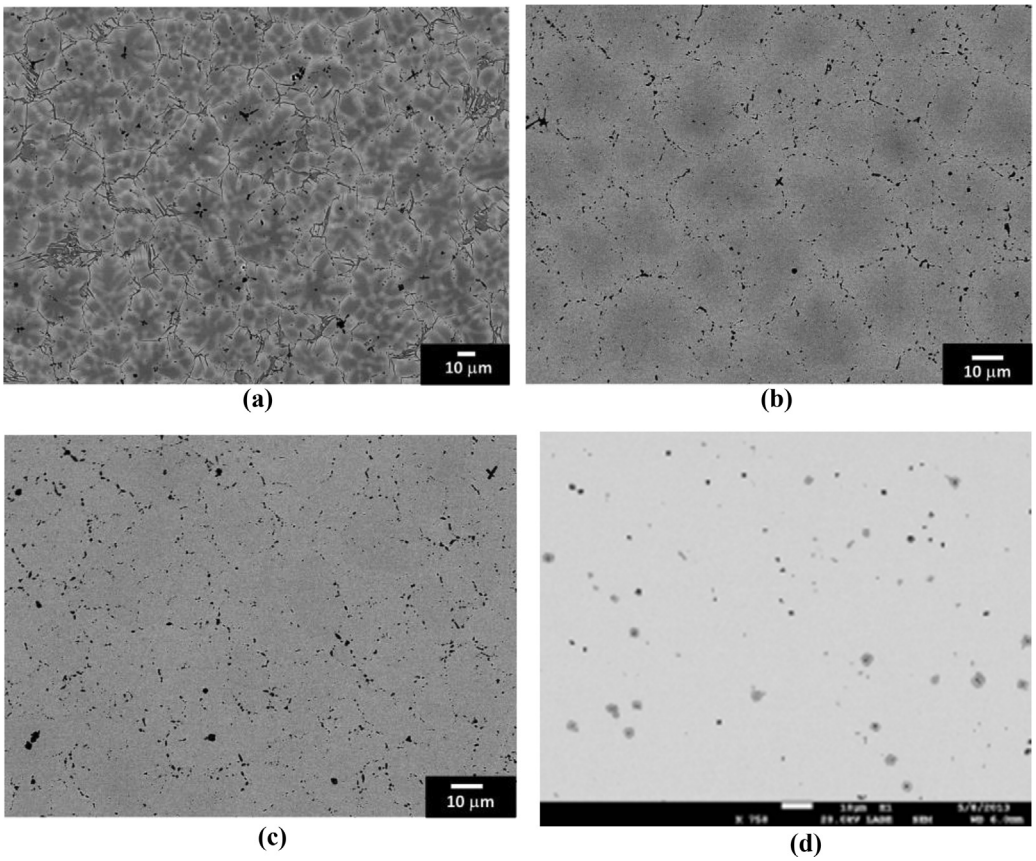

Fig. 1. BSE-SEM images of the U-22at%Mo (U–10Mo) samples: (a) as-cast sample; (b–c) homogenized at 800 °C for 4 and 24 h; and (d) homogenized at 1000 °C for 16 h, respectively; Corresponding grain size was measured as 25–30 μm for (a–c) and approximately 200–250 μm for (d). Notice that the intensity of the dark gray areas (Mo-segregation/Mo-rich regions) decreases as the homogenization time and temperature increase. The black phases are carbides of uranium.

was determined based on the BSE atomic number contrast (Z contrast) and EDS line scans (Fig. 2). It should be noted that the Z contrast is directly proportional to molybdenum variation observed in the line scan data. However it should also be noted that the direct correlation between the molybdenum concentration in BSE-SEM image and EDS line scans is dependent on the operator and machine settings. This technique will only be valid if EDS line scans are drawn on the given sample condition of U–10Mo. This technique is an extension of Snyder's work [6] and attempts to incorporate the overall microstructure to predict the homogenization kinetics.

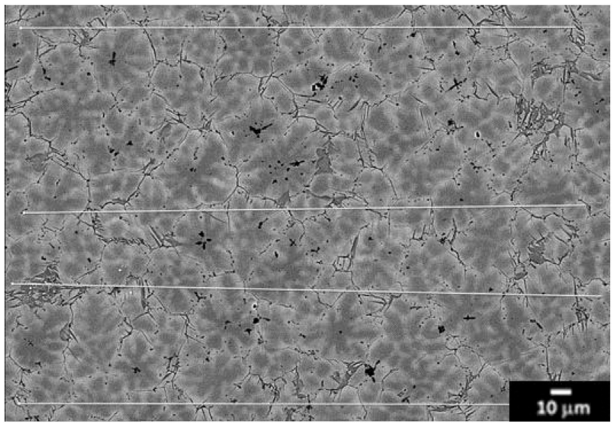

Fig. 2. EDS line scans where Mo concentration is sampled and line scan data is collected in Fig. 1a (BSE-SEM image).

The sample homogenized at 800 °C for 24 h had a variable grain size distribution, with the grain size varying from 10 to 30 μm. The other important aspect was that the carbides for the samples homogenized at 1000 °C for 16 h were spherical with diameters up to 8 μm in some cases and were located within the grain, unlike the samples heat treated at 800 °C for 24 h, in which all carbides were found at the grain boundaries. The shape change and coarsening of the spherical carbides can likely be associated with Ostwald ripening [24]. The carbides present in the U–10Mo samples homogenized at 800 °C for 24 h had an aspect ratio of 1:5, with the largest diameter being approximately 1–2 μm, and were located primarily at the grain boundaries.

3. Modeling the homogenization kinetics

3.1. Homogenization model and quantitative measurement of homogenization

The homogenization model provides the governing equation describing the diffusion-induced dissolution of segregated molybdenum. The proposed model considers the diffusion of Mo in U–10Mo,

$$\frac{\partial c}{\partial t} = \nabla(D\nabla c), \tag{1}$$

where $c(\boldsymbol{x},t)$ is the atomic concentration of Mo at given location $\boldsymbol{x}$ and time t. Mo intrinsic diffusivity is dependent on the Mo

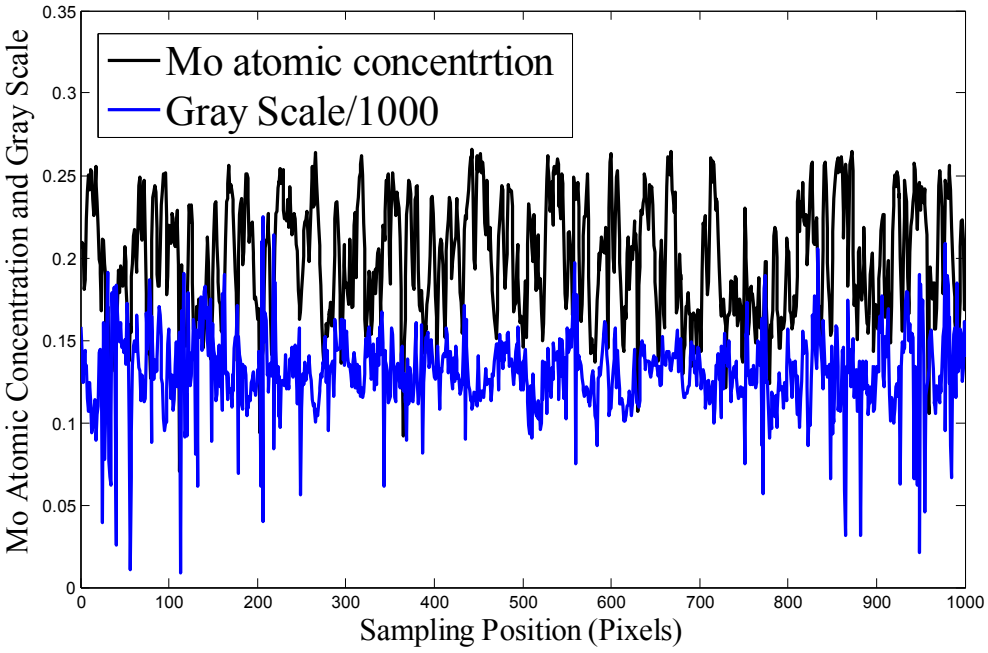

Fig. 3. EDS Line scan data of gray scale and Mo concentration for the typical sample shown in Fig. 2.

concentration and D is the effective diffusion constant of Mo at the temperature of homogenization (800 °C and 1000 °C in this study). Similar to the method used by Snyder [10,11], the initial Mo concentration with segregation can be approximated by a sine function.

$$c(\mathbf{x}, t=0) = c_0 + A\sin\left(\frac{\pi x}{l_x}\right)\sin\left(\frac{\pi y}{l_y}\right)\sin\left(\frac{\pi z}{l_z}\right), \tag{2}$$

where c_0 is the nominal Mo concentration in U–Mo alloys and x, y and z are three Cartesian coordinates. A represents the amplitude of Mo concentration fluctuation, as the difference between maximum and minimum Mo concentration can be written as $2A$. Three characteristic length scales, l_x, l_y, and l_z, denote the period of concentration fluctuation along each coordinate that can be related to the grain size in each direction.

The analytical solution of Eq. (1) with initial condition of Eq. (2) can be shown as

$$c(\mathbf{x}, t) = c_0 + A\cdot\exp\left(-\frac{\pi^2 Dt}{l_0^2}\right)\sin\left(\frac{\pi x}{l_x}\right)\sin\left(\frac{\pi y}{l_y}\right)\sin\left(\frac{\pi z}{l_z}\right), \tag{3}$$

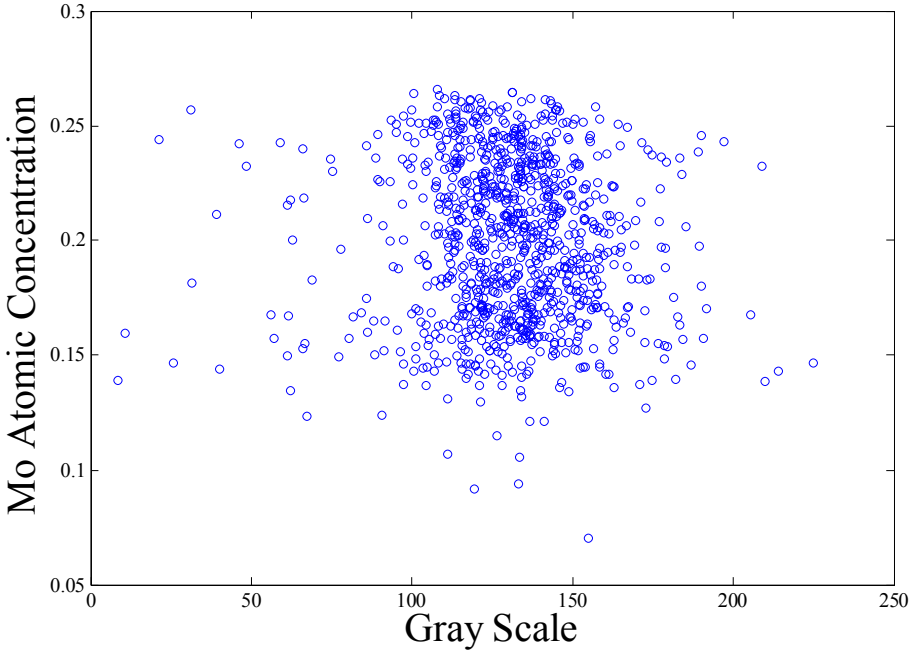

Fig. 4. Pointwise plot of correlation between Mo concentration and gray scale.

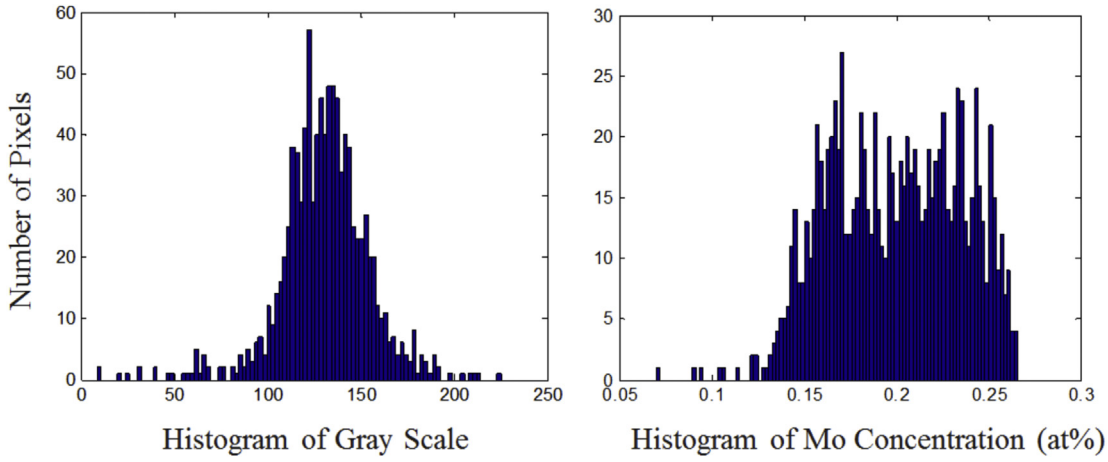

Fig. 5. Histograms of gray scale and Mo weight concentration (at%) from line scan data.

where the newly introduced characteristic length l_0 is defined as

$$\frac{1}{l_0^2}=\frac{1}{l_x^2}+\frac{1}{l_y^2}+\frac{1}{l_z^2}. \tag{4}$$

It was found from Eq. (3) that the effective length scale l_0 controls the kinetic rate of homogenization, where a larger l_0 leads to slower homogenization. The value of l_0 is essentially dominated by the smallest length scale of l_x, l_y, and l_z from Eq. (4).

At any instant t, the difference between maximum and minimum concentration can be written as

$$\Delta c = c_{\max}-c_{\min}=2A\exp\left(-\frac{\pi^2 Dt}{l_0^2}\right) \tag{5}$$

from Eq. (3), or equivalently in the logarithmic form

$$\log_{10}(\Delta c)=\log_{10}(c_{\max}-c_{\min})=\log_{10}(2A)-\frac{\pi^2 Dt}{l_0^2}\log_{10}(e), \tag{6}$$

Equation (5) indicates that the concentration difference Δc follows an exponential decrease with time and the rate constant is related to the diffusion constant D and the effective length scale l_0. Solution (3) has been derived based on the much-idealized approximation (Eq. (2)) of Mo segregation. Hence, the true homogenization kinetics might deviate from Eq. (5) because of this approximation. Δc will be used as a quantitative measurement of the degree of homogenization.

3.2. Reconstruction of Mo concentration field from BSE-SEM images

During the thermomechanical process optimization of U-10wt% Mo, room temperature x-ray diffraction (XRD) and SEM combined with EDS have been used to characterize the material structures of as-cast and homogenized samples. Elemental mapping from EDS has indicated the bulk chemical inhomogeneity for molybdenum, carbon, oxygen and silicon. Fig. 2 shows the Mo segregation in INL pin casting samples with Mo concentrated in intra-dendritic regions (dark color) and lean in Mo in inter-dendritic and grain boundary regions (light color).

The purpose of Mo concentration reconstruction is to

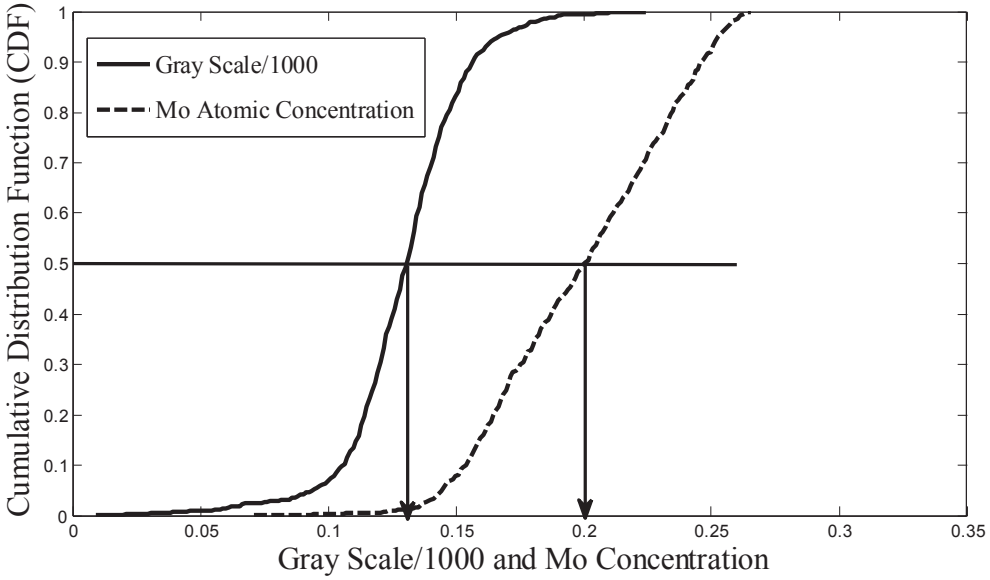

Fig. 6. Cumulative distribution functions of image gray scale (thick solid line) and Mo atomic concentration (dashed line) from line scan data.

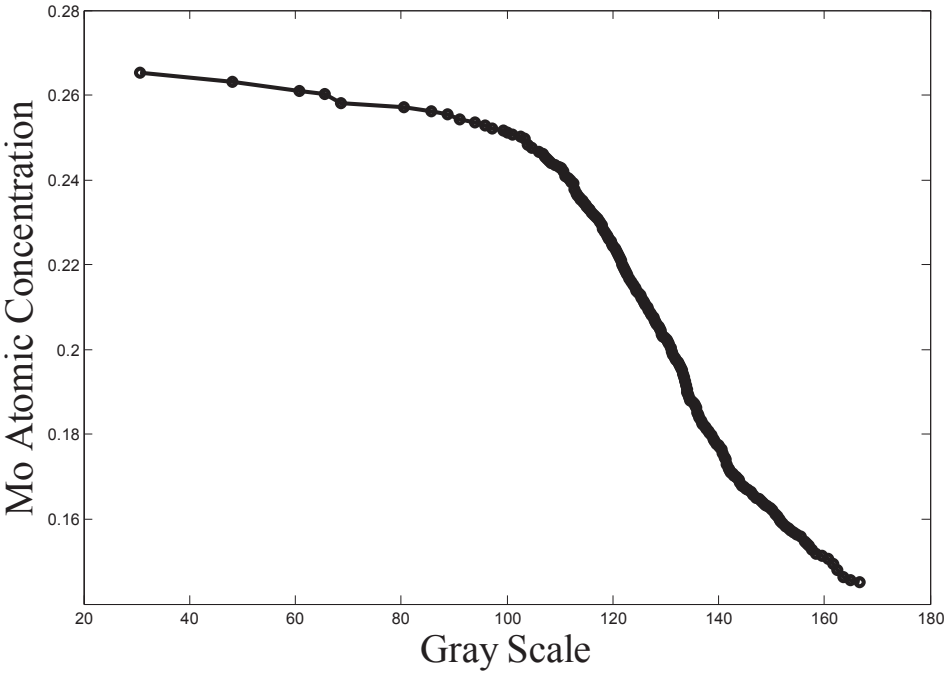

Fig. 7. Nonlinear relationship between the image gray scale and Mo atomic concentration.

reconstruct the Mo concentration distribution from experimental EDS and BSE-SEM images. The reconstructed Mo concentration map for as-cast samples before homogenization can be used as the input for Mo homogenization simulations to predict the entire homogenization kinetics. The information extracted from BSE-SEM images at different times can be compared to and validate the Mo homogenization kinetics obtained from numerical simulations.

In order to reconstruct the Mo concentration map from BSE-SEM images, line scan data from EDS is needed to provide accurate correlations between the gray scale and Mo concentration. Fig. 2 shows the locations of lines where Mo concentration was sampled in this particular image to provide the line scan data of Mo concentration. Fig. 3 shows the gray scale and Mo concentration for each sampling point along all the EDS lines. It was found that in general, lower gray scale corresponds to higher Mo concentration except at those points within carbide particles with low gray scale and low Mo concentration.

In order to identify the dependence of Mo concentration on the image gray scale (BSE-SEM image), we first plot the pointwise Mo concentration vs. the gray scale based on the line scan data from Fig. 3. This plot is presented in Fig. 4, which does not exhibit a unique and obvious relationship between Mo concentration and the gray scale. Hence we proposed a new method to extract this important relationship from BSE-SEM images, which is described in detail as follows:

1. The histograms of gray scale and Mo concentration from the line scan data in Fig. 3 are plotted in Fig. 5. The two histograms show similar patterns (close to Gaussian distribution).

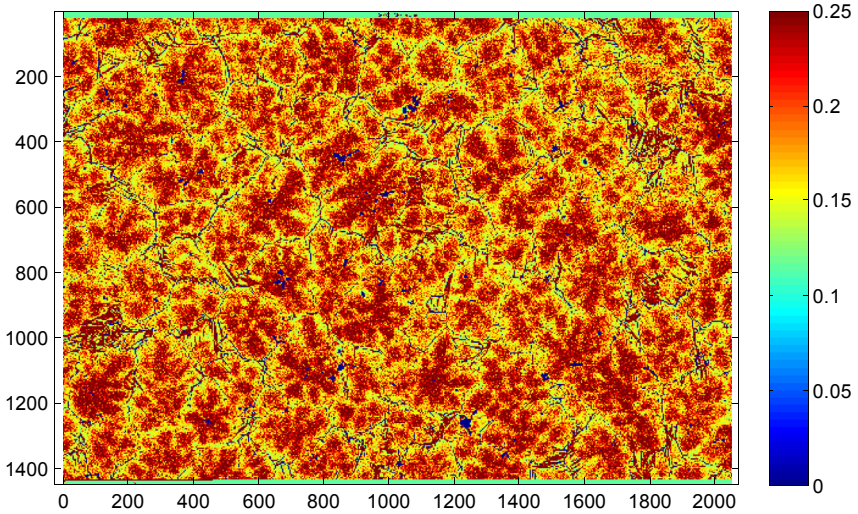

Fig. 8. Reconstructed Mo concentration map corresponding to the BSE-SEM image in Fig. 2. Axis units are the number of pixels.

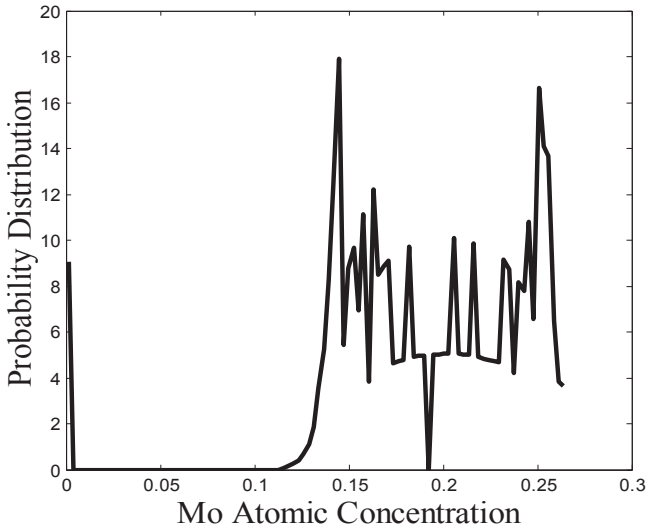

Fig. 9. Probability distribution of Mo atomic concentration from reconstructed Mo concentration map corresponding to the BSE-SEM image in Fig. 2.

2. The cumulative distribution functions (CDFs) for both gray scale and Mo concentration are plotted in Fig. 6. Both CDFs are smooth functions increasing from 0 to 1.
3. Mo atomic concentration and image gray scale can be identified for each percentage along the vertical axis in CDF plots (Fig. 6). Plotting the concentration as a function of the gray scale found from Fig. 6 gives the nonlinear relation between Mo concentration and image gray scale shown in Fig. 7.
4. The Mo concentration map of the entire image can be obtained by reading the BSE-SEM image and converting the gray scale to the Mo concentration pixel by pixel based on the nonlinear relationship from Fig. 7. For this particular example, the Mo concentration map for the BSE-SEM image in Fig. 2 is presented in Fig. 8. The Mo segregation can be clearly observed in the reconstructed Mo concentration map with Mo-rich regions in red color and Mo-lean regions in blue color.
5. The probability distribution and cumulative distribution of Mo atomic concentration are plotted in Figs. 9 and 10, respectively, from the Mo concentration map (Fig. 8). The two peaks around Mo concentration of 0.15 and 0.25 in the probability distribution plot clearly indicate the Mo-rich and -lean regions, respectively.
6. A quantitative measure of the degree of homogenization can be identified from the cumulative probability plot of Mo concentration in Fig. 10. Based on the analytical solution in Eq. (3), Δc (the difference between maximum and minimum Mo concentration) is introduced as the quantitative measure of homogenization. The analytical solution indicates that Δc decreases exponentially with homogenization time. The smaller Δc, the more homogenized the Mo. In practice, Δc is defined as

$$\Delta c = 2(c_{95\%} - c_{50\%}), \tag{7}$$

where c_p is the concentration at which the probability $P(c < c_p) = p$ *and* p can be 95% or 50% in Eq. (7).

3.3. Numerical method to solve the homogenization model

The formation of inhomogeneous dendritic structure in U–10Mo as-cast microstructure is quite complex that can be simulated in principle by some advanced numerical methods [25–27] designed for moving interface problems [28]. The purpose of Mo homogenization modeling is to provide time-evolving kinetics of the degree of homogenization at given temperatures. Only the diffusion mechanism will be simulated in this work. A reconstructed Mo concentration map of as-cast samples (Fig. 8) will be used as the input of a representative realistic initial Mo concentration field. Mo homogenization simulations are implemented by solving the homogenization equation (Eq. (1)) using a two-dimensional finite-difference code.

Since the resolution of BSE-SEM images is about 0.1 μm per pixel, the simulation domain of 1.2 mm × 1.6 mm consists of 1200 × 1600 grids with the grid size the same as the pixel size. A finite-difference

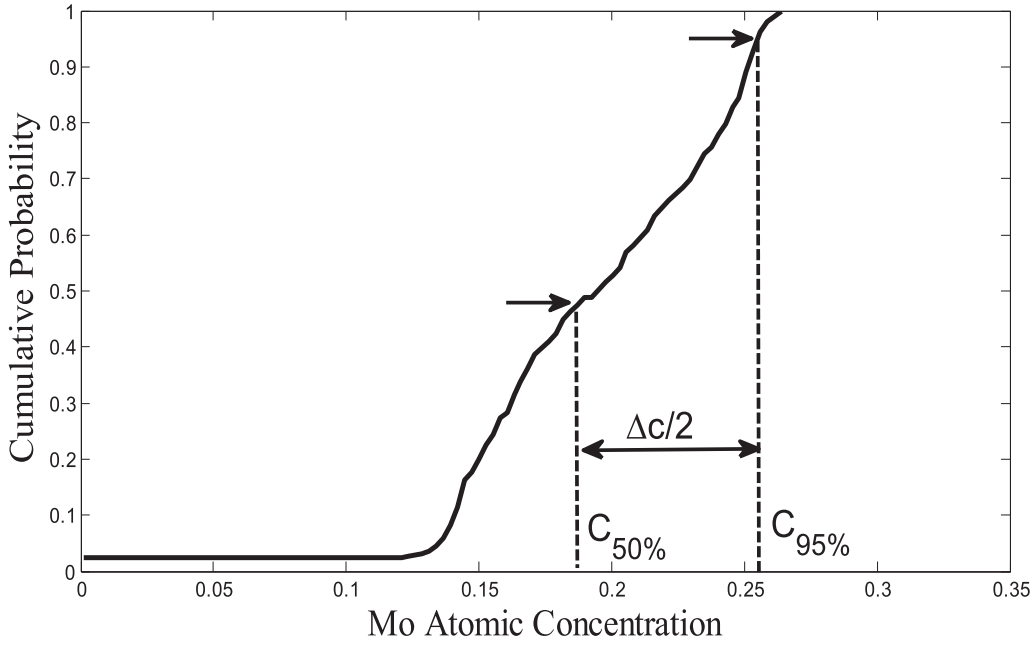

Fig. 10. Cumulative distribution of Mo atomic concentration from reconstructed Mo concentration map (Fig. 8) corresponding to the BSE-SEM image in Fig. 2.

scheme was used to discretize the domain and approximate the first-order and second-order derivatives for the homogenization equation (Eq. (1)). Discretization in time is written as,

$$\frac{\partial c}{\partial t} = \frac{c^{t+\Delta t} - c^{t}}{\Delta t}, \tag{8}$$

where Δt is the time step and c^t is the Mo concentration at current time t. The Laplacian in homogenization equations is computed from the commonly used five-point finite-difference stencil,

$$\nabla^2 c_{i,j} = \frac{c_{i+1,j} + c_{i-1,j} + c_{i,j+1} + c_{i,j-1} - 4c_{i,j}}{\Delta x^2}. \tag{9}$$

where Δx is grid size and $c_{i,j}$ is the Mo concentration at the grid point with index (i, j).

The time variation of Δc, e.g. the quantitative measure of homogenization, is the output from the homogenization simulations, which can be directly compared to the same measure from BSE-SEM images at different homogenization times and temperatures.

4. Results and discussion

4.1. Reconstructed Mo concentration map from EDS images

The methodology for reconstruction of Mo concentration maps from BSE-SEM images and line scan data was described in Section III. By applying this methodology to BSE-SEM images of as-cast and homogenized samples, we are able to reconstruct the Mo concentration field and extract quantitative measures of Δc for all BSE-SEM images at different homogenization times and temperatures.

The nonlinear relation between the BSE-SEM combined with EDS line scans and Mo atomic concentration can be obtained by following the procedures in Section III. This relation shows significant difference for different BSE-SEM images due to different contrast and brightness recorded. With this nonlinear relation obtained for any particular BSE-SEM image at different homogenization time, Fig. 11 presents reconstructed Mo concentration maps at 4 h, 8 h, 16 h, 24 h, and 48 h at the temperature of 800 °C. The process of homogenization with time was shown with the

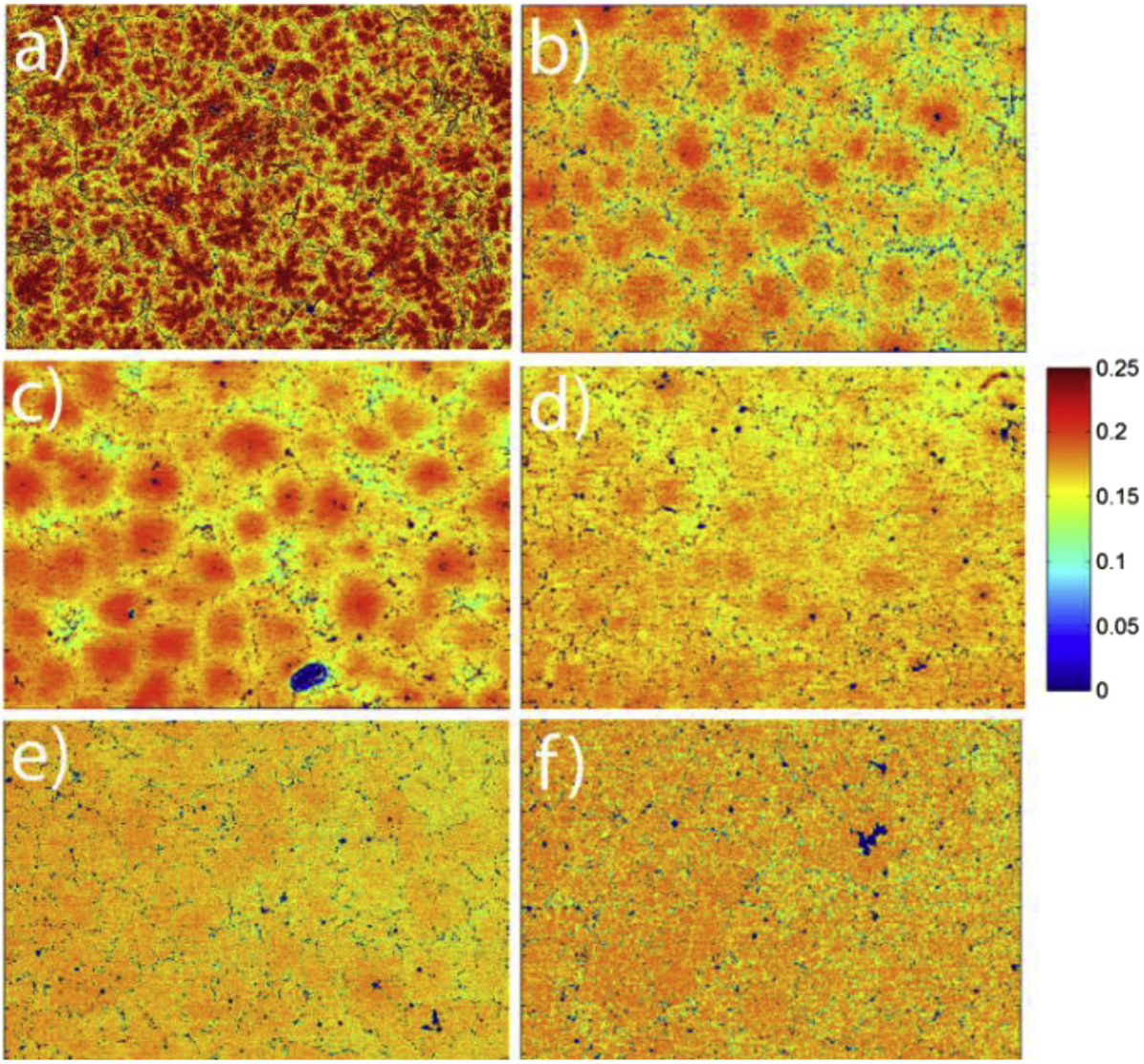

Fig. 11. Reconstructed distribution of Mo atomic concentration from BSE-SEM images at various homogenization times and temperatures (corresponding to BSE-SEM images in Fig. 2): a) INL as-cast pin sample; b) homogenized 4 h at 800 °C; c) homogenized 8 h at 800 °C; d) homogenized 16 h at 800 °C; e) homogenized 24 h at 800 °C; f) homogenized 48 h at 800 °C.

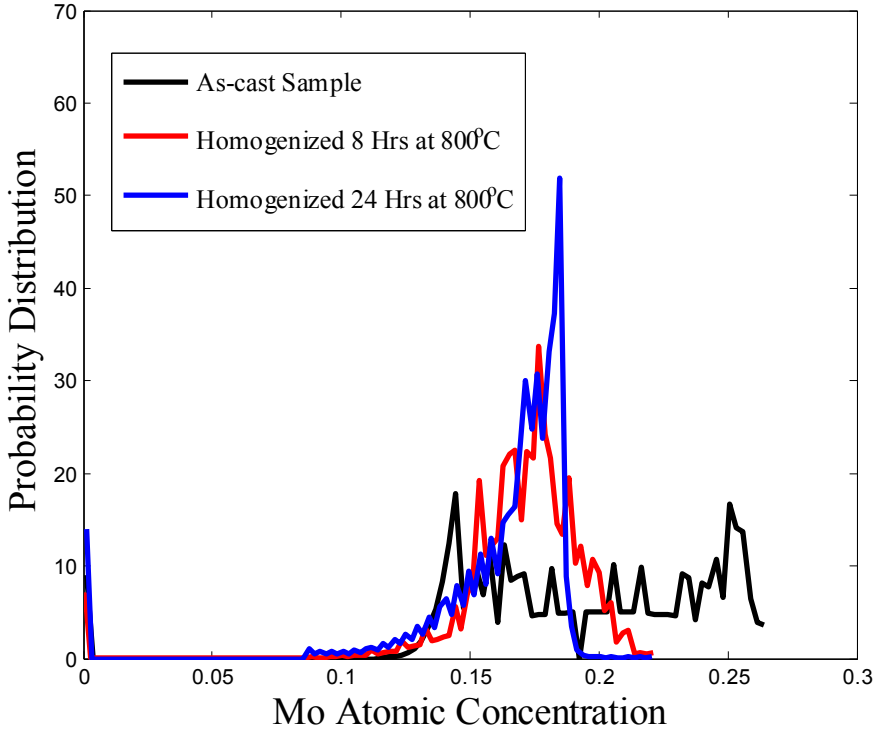

Fig. 12. Probability distribution of Mo atomic concentration for reconstructed Mo concentration map from BSE-SEM images of samples homogenized at 800 °C for various times.

dissolving of clusters with high Mo concentration. The carbide particles are represented by blue regions with zero Mo concentration. The morphology of carbide particles is well preserved in the reconstructed concentration maps. The inhomogeneity of Mo distribution with Mo-rich and -lean regions can be clearly identified in the reconstructed concentration maps. The reconstructed concentration map of an as-cast sample was used as the initial concentration field for simulations of homogenization kinetics.

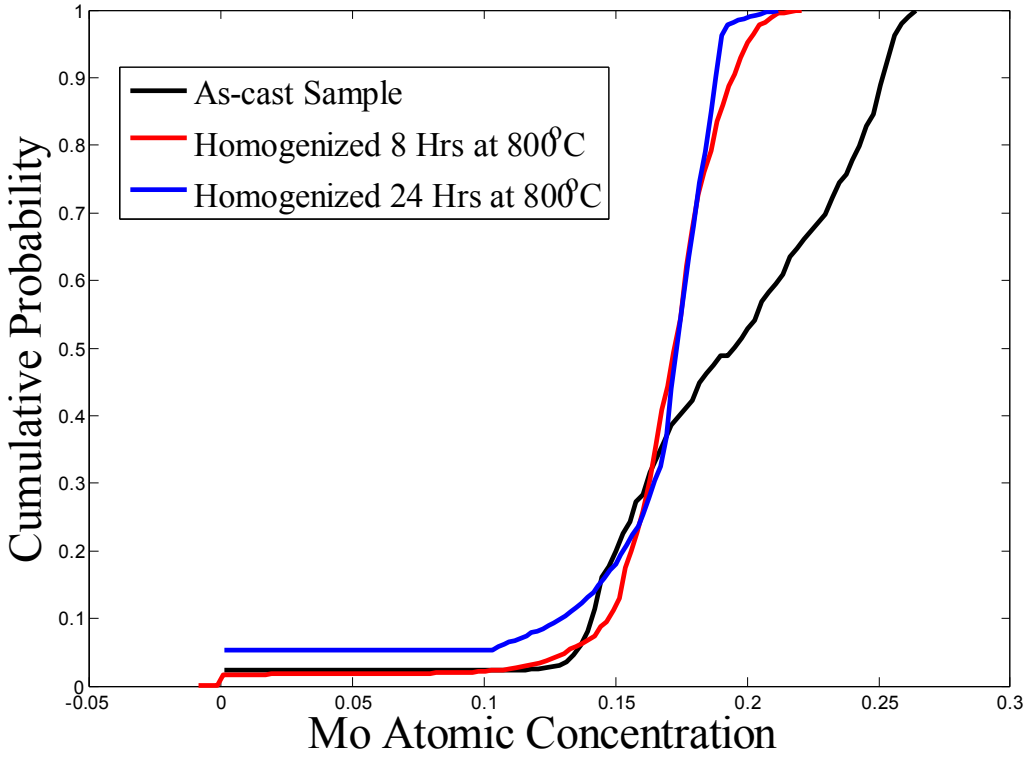

Fig. 13. Cumulative probability distribution of Mo atomic concentration for reconstructed Mo concentration map from BSE-SEM images at 800 °C for various homogenization times.

Fig. 12 gives the statistical information of Mo concentration based on the reconstructed concentration map. Three peaks in the probability distribution of Mo concentration for as-cast sample (Fig. 12) correspond to the fraction of carbide particles (2%), the Mo atomic concentration next to the grain boundary (15%), and the Mo atomic concentration in dendrite (25%). The cumulative distribution function of Mo concentration in Fig. 13 shows a very wide distribution of Mo atomic concentration from 13% to 26%, indicating a very inhomogeneous Mo distribution in as-cast samples.

The probability distribution in Fig. 12 from the Mo concentration map shows that the homogenization process merges the two peaks in the as-cast samples into a single peak of atomic concentration around 17%. During the homogenization process, the diffusion of Mo leads to a more uniform Mo distribution. The quantitative measure introduced in Section 3 can be calculated from the cumulative distribution of Mo concentration.

4.2. Mo homogenization kinetics

With the reconstructed Mo concentration map in Fig. 8 and the simulation method described in Section III, we have implemented the homogenization simulations to simulate the homogenization kinetics. The quantitative measure Δc for homogenization can be obtained both from simulations and from experimental BSE-SEM images at different homogenization times and temperatures. The direct comparison between simulations and experiments is presented in Fig. 14, where square symbols represent the quantitative measure from experiments at 800 °C for pin casting samples, and line for the homogenization simulations with the reconstructed concentration map of the as-cast sample as the input. Both experiment and simulation show the trend of homogenization with decreasing quantitative measure Δc. The diffusion coefficient used for Mo diffusion was chosen as $D = 10^{-16}$ m^2/s to fit the simulated homogenization kinetics. The Mo intrinsic diffusivity in U–10Mo is non-uniform and highly dependent on the local Mo concentration. Based on the limited study in Mo diffusivity [29,30], the estimated Mo diffusivity in U–10Mo at 800 °C can be ~1.8×10^{-16} m^2/s which is larger compared to the value chosen. The discrepancy may be understood as the non-uniform distribution of Mo in U–10Mo.

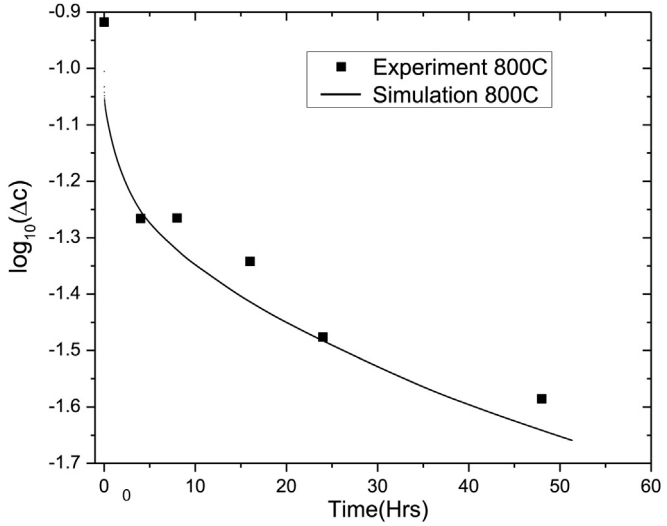

Fig. 14. Homogenization kinetics from simulation (line) and experimental BSE-SEM images (squares for 800 °C).

5. Conclusion

Mo concentration of pin-cast samples with grain sizes 25–30 μm at various homogenization times have been characterized by BSE-SEM images. EDS Line scan data of Mo concentration was obtained from these BSE-SEM images. A novel numerical procedure was developed to correlate the Mo concentration with image gray scale, such that a complete Mo concentration map can be established from BSE-SEM images. A quantitative measure of the degree of homogenization was identified from the analytical study. This measure can be computed for BSE-SEM images of samples with various homogenization times to quantitatively describe the kinetics of Mo homogenization. A kinetic model was presented to simulate the Mo homogenization kinetics, with Mo concentration reconstructed from an as-cast sample as the initial concentration. The model was validated by comparison between simulated homogenization kinetics and the results from BSE-SEM images for pin-cast samples. This predictive capability can be further extended to study the homogenization of U–10Mo with various grain sizes and non-equiaxed grains that are common in thermomechanically processed material.

Acknowledgments

The current work was supported by the DOE National Nuclear Security Administration under Contract DE-AC05-76RL01830. The authors would like to acknowledge Dongsheng Li for his preliminary inputs for this work. The authors would also like to thank Crystal Rutherford, Anthony Guzman, Danny Edwards and Alan Schemer-Kohrn of Pacific Northwest National Laboratory for assisting in the microstructural characterization, and all the other staff directly or indirectly associated with producing the results. The authors also thank Mr. Glenn Moore, Mr. Brady Mackowiak, Mr. Steve Steffler and Mr. Jason Schulthess of INL for fabrication and supply of the U–10Mo test samples.

References

[1] M.K. Meyer, et al., Low-temperature irradiation behavior of uranium-molybdenum alloy dispersion fuel, J. Nucl. Mater. 304 (2–3) (2002) 221–236.
[2] J.L. Snelgrove, et al., Development of very-high-density low-enriched-uranium fuels, Nucl. Eng. Des. 178 (1) (1997) 119–126.
[3] D.D. Keiser, et al., High-density, low-enriched uranium fuel for nuclear research reactors, Jom J. Miner. Metals Mater. Soc. 55 (9) (2003) 55–58.
[4] Joshi, V.V., et al., Thermomechanical process optimization of U-10wt% Mo – Part 1: high-temperature compressive properties and microstructure. J. Nucl. Mater., (0).
[5] E. Nyberg, et al., The Influence of Casting Conditions on the Microstructure of As-cast U-10Mo Alloys: Characterization of the Casting Process Baseline, PNNL-23049, Pacific Northwest National Laboratory, Richalnd, WA, 2013.
[6] V.V. Joshi, et al., Thermomechanical process optimization of U-10wt% Mo – Part 2: the effect of homogenization on the mechanical properties and microstructure, J. Nucl. Mater. 465 (2015) 710–718.
[7] E.A. Nyberg, et al., The Influence of Homogenization on the Mechanical Properties and Microstructure on U-10Mo Alloy, PNNL-23348, Pacific Northwest National Laboratory, Richland WA, 2013.
[8] W.A. Bostrom, E.K. Halteman, The Metastable Gamma Phase In Uranium Base Molybdenum Alloys, 1956. Other Information: Orig. Receipt Date: 31-DEC-58. p. Medium: ED; Size: Pages: 32.
[9] D.E. Burkes, et al., Properties of DU–10 wt% Mo alloys subjected to various post-rolling heat treatments, Nucl. Eng. Des. 240 (6) (2010) 1332–1339.
[10] W.B. Snyder, in: O.R.Y. Plant (Ed.), Effects of Heat Treatment on the Microstructure and Mechanical Properties of U-6Nb Alloy, 1978. Oak Ridge Tennessee.
[11] W.B. Synder, Homogenization of Arc-melted U-6Nb Alloy Ingots, Oak Ridge Y-12 Plat, Oak Ridge, Tennessee, 1978.
[12] D.A. Lopes, et al., Gamma-phase homogenization and texture in U–7.5Nb–2.5Zr (Mulberry) alloy, J. Nucl. Mater. 449 (1–3) (2014) 23–30.
[13] D.A. Porter, K.E. Easterling, M. Sherif, Phase Transformations in Metals and Alloys, Revised Reprint, third ed., Taylor & Francis, 2009.
[14] Q. Du, et al., Microstructure evolution during homogenization of Al–Mn–Fe–Si alloys: Modeling and experimental results, Acta Mater. 61 (13) (2013) 4961–4973.

[15] R.D. Lanam, R.W. Heckel, A study of the effect of an intermediate phase on the dissolution and homogenization characteristics of binary alloys, Metall. Mater. Trans. B 2 (8) (1971) 2255–2266.
[16] Z.-w. Chen, S.-s. Li, J. Zhao, Homogenization of twin-roll cast A8006 alloy, Trans. Nonferr. Metals Soc. China 22 (6) (2012) 1280–1285.
[17] M. Jia, Z. Zheng, Z. Gong, Microstructure evolution of the 1469 Al–Cu–Li–Sc alloy during homogenization, J. Alloys Compd. 614 (0) (2014) 131–139.
[18] A. Yamanaka, T. Takaki, Y. Tomita, Coupled simulation of microstructural formation and deformation behavior of ferrite–pearlite steel by phase-field method and homogenization method, Mater. Sci. Eng. A 480 (1–2) (2008) 244–252.
[19] R.C. Kramb, M.M. Antony, S.L. Semiatin, Homogenization of a nickel-base superalloy ingot material, Scr. Mater. 54 (9) (2006) 1645–1649.
[20] R.M. Nekkanti, P.A. McQuay, S.L. Semiatin, Measurement of homogenization kinetics for a near-gamma titanium aluminide, Scr. Metall. Mater. 26 (7) (1992) 1089–1094.
[21] S.L. Semiatin, et al., Analysis of the homogenization of a nickel-base superalloy, Scr. Mater. 51 (6) (2004) 491–495.
[22] D.J. Edwards, et al., Characterization of U-mo Foils for AFIP-7, PNNL-21990, Pacific Northwest National Laboratory, Richland, WA, 2012.
[23] Amy Clarke, et al., Microstructure characterization and processing of U-Mo alloy fuels for nuclear reactors, in: TMS Annual Meeting & Exhibition, Characterization of Nuclear Reactor Materials and Components with Neutron and Synchrotron Radiation 2011. San Diego, 2011.
[24] L. Ratke, P.W. Voorhees, Growth and Coarsening: Ostwald Ripening in Material Processing, Springer, 2002.
[25] Z.J. Xu, et al., Phase field and level set methods for modeling solute precipitation and/or dissolution, Comput. Phys. Commun. 183 (1) (2012) 15–19.
[26] Z. Xu, P. Meakin, A phase-field approach to no-slip boundary conditions in dissipative particle dynamics and other particle models for fluid flow in geometrically complex confined systems, J. Chem. Phys. 130 (23) (2009) 234103.
[27] Z. Xu, P. Meakin, Phase-field modeling of two-dimensional solute precipitation/dissolution: solid fingers and diffusion-limited precipitation, J. Chem. Phys. 134 (4) (2011) 044137.
[28] Z.J. Xu, K.M. Rosso, S. Bruemmer, Metal oxidation kinetics and the transition from thin to thick films, Phys. Chem. Chem. Phys. 14 (42) (2012) 14534–14539.
[29] Y. Adda, J. Philibert, Study the kirkendall effect and determination of the chemical and intrinsical diffusion coefficients in the couple U-Mo, Comptes Rendus 246 (1958) 113.
[30] K. Huang, D.D. Keiser, Y.H. Sohn, Interdiffusion, intrinsic diffusion, atomic mobility, and vacancy wind effect in gamma(bcc) uranium-molybdenum alloy, Metall. Mater. Trans. A Phys. Metall. Mater. Sci. 44A (2) (2013) 738–746.